# In-situ Characterization of Nanopowders During Compaction Using SANS and AC Impedance Spectroscopy

Thomas J. Rudzik and Rosario A. Gerhardt*

*Georgia Institute of Technology, Atlanta, GA, USA, rosario.gerhardt@mse.gatech.edu

## ABSTRACT

Sintering is one of the primary methods of fabrication of ceramic materials, so a detailed understanding of the processing-property relationships for materials undergoing sintering is of great potential value. A new testing method combining small angle neutron scattering (SANS) and ac impedance spectroscopy (IS) during the compaction of ceramic powders has been developed to track the evolution of the powder compact microstructure throughout the compaction process. IS and SANS data for multiple ceramic powders exhibited the expected trends, with resistivity and porosity decreasing as applied pressure increased. The similarities between the SANS and IS data trends show that the tests were successful in tracking the changing microstructure of the powders. Therefore, these tests were a successful proof of concept of this powerful new characterization technique. In the future, heating will be incorporated to apply this technique to the actual sintering processes.

***Keywords***: SANS, impedance spectroscopy, porosity, sintering, ceramic powders

## 1 INTRODUCTION

Sintering is one of the most commonly used processing methods for the fabrication of bulk ceramics. Therefore, detailed knowledge of how the sintering process affects the final properties of ceramics has a high potential value to a wide range of industries, which would benefit from the ability to tune the properties of ceramics to desired values through the knowledge of these relationships. The properties of materials are highly dependent on their microstructures, so an understanding of how the sintering process evolves the microstructure of a powder is important in facilitating the design of ceramics and in the development of process models [1, 2]. The microstructure of the powder at any point during the sintering process affects the mechanisms which drive further sintering [2, 3]. The dominant microstructural feature in homogeneous powders is the pore structure, which is, therefore, the primary focus of the current investigation, because knowledge of the pore structure at each point in the sintering process will ultimately give insight into how the microstructure and properties evolve.

Some of the most useful methods for the characterization of porous microstructures are small angle scattering tests, which have gained recognition due to their non-destructive nature and the variety of data they can provide, including number and volume fractions of pores, the surface areas of both open and closed pores, the pore size distribution, and the topology of the microstructure [4-6]. Small angle neutron scattering (SANS) can characterize features in the size range of 1 nm to 0.1 μm and is, therefore, ideal for studying a wide range of microstructural features [2, 6].

As powder particles deform during sintering, the nature of the interfaces between them changes from point contact of undeformed particles in the initial stages to contact between fully sintered particles in the final stages [3]. The electrical properties of a material are very sensitive to changes in the interfaces between particles, making electrical characterization a useful tool for evaluating the evolution of the microstructure during sintering [7]. Ac impedance spectroscopy (IS) is a versatile electrical characterization method which can be used to develop equivalent circuit models for a material, which can be used to separate the electrical responses of the pores and the bulk material [8] and to identify the types of interfaces present between the particles [9]. This was recently demonstrated in an ex-situ study on a series of glass composites containing conducting fillers at the interstices between the glass particles [7]. Therefore, IS can be used to track microstructural evolution during sintering by detecting the changes in particle-particle interfaces associated with the sintering of the powder.

Although ex-situ IS studies have been conducted in the past [10], combining the porosity characterization provided by SANS with the simultaneous interfacial characterization of IS has not been attempted before. Doing so will give a complete and detailed picture of the microstructure at any stage of sintering. The data from this test will identify correlations between SANS measurements and the densification mechanisms in the material, so after SANS test are conducted, ex-situ IS tests could be used to track the sintering behavior.

## 2 EXPERIMENTAL PROCEDURE

Approximately 0.3g of three ceramic powders, indium tin oxide (ITO) nanopowder (Inframat Advanced Materials, Manchester, CT), antimony tin oxide (ATO) nanopowder (Alfa Aesar, Ward Hill, MA), and micron-sized β-SiC powder (Alfa Aesar, Ward Hill, MA), were measured and placed into the die assembly shown in figure

1. The powder was contained in a sapphire die with titanium spacers in both ends and an aluminum shroud around the die. The shroud acted as a safety measure in case the die were to rupture. The spacers separated the powder from the custom-made steel punches such that even in the most compressed state, the punches did not enter the path of the neutron beam. This is important because the steel punches strongly absorb neutrons, whereas the sapphire die, aluminum shroud, and titanium spacers are all transparent to neutrons. Electrical leads were attached to the outer edges of the large disk sections of the punches, and wires from the IS equipment were attached to these leads. Therefore, the current applied during the IS measurements travelled from the IS equipment through the steel punch, titanium spacers, powder sample, other titanium spacers, the other steel punch, and back to the equipment. The die assembly was attached to a tension-to-compression fixture, separated by wood spacers to electrically isolate the die assembly and steel spacers to adjust the position of the die assembly to get the powder directly into the neutron beam path. The tension to compression fixture was used to convert the tensile force applied by the computer-controlled load frame to a compressive force on the steel punches. This fixture was secured within the load frame, which was mounted in the path of the GP-SANS beamline [11] at the HFIR facility at Oak Ridge National Laboratory (ORNL) (Fig. 2). It was mounted such that the direction of applied pressure made an angle of 45° with the neutron beam direction in order to increase the volume of powder in the beam path.

The impedance tests were conducted as a continually-looping frequency sweep from 10 MHz to 0.1 Hz with a constant ac voltage of 500 mV. The looping program was started before the first SANS test on a sample started and continued running until the final SANS test on that sample ended. After the IS tests were started, the load

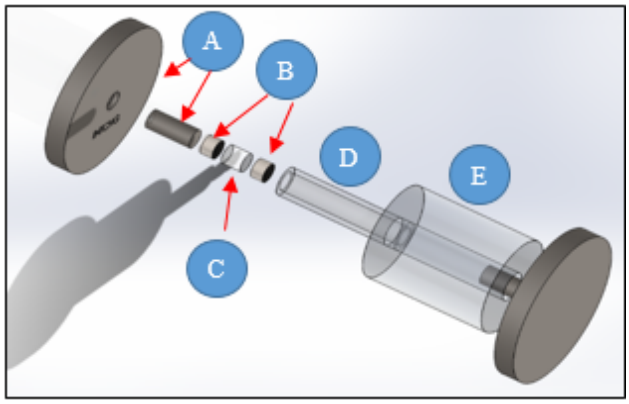


Figure 1: An exploded view of the compression die main assembly. The punches (A), consisting of steel cylinders protruding from large steel discs, apply pressure from the load frame through the titanium spacers (B) to the ceramic powder (C). The powder and titanium spacers are contained within the sapphire die (D), which fits within the aluminum shroud (E). Picture courtesy of Paris Cornwell at ORNL.

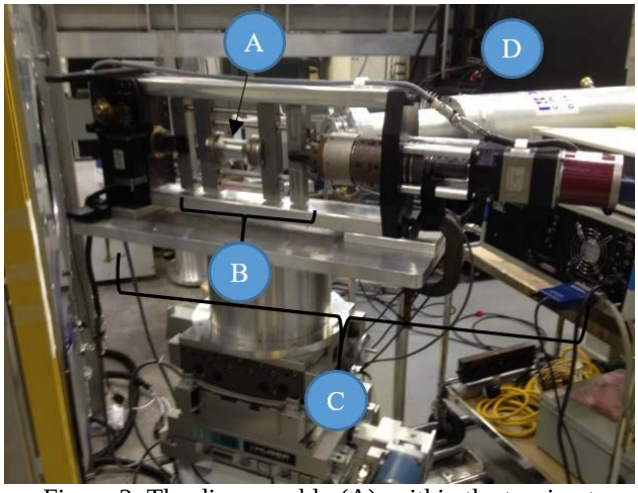


Figure 2: The die assembly (A), within the tension to compression fixture (B), within the load frame (C), mounted in the path of the GP-SANS beamline (D) at the HFIR facility at ORNL [11].

frame displaced the punches until both made full contact with the powder, indicated by the measured pressure starting to increase. The first set of SANS tests were then run at this pressure condition under the designation 0 MPa. SANS testing for each sample was conducted at each of a series of discreet applied pressures ranging from 0 to 300 MPa at 50 MPa increments and consisted of three separate SANS measurements, where one was made at a sample to detector distance (S-D) of 2 m to measure larger scattering angles, one at a S-D of 18.5 m to measure smaller scattering angles, and one at a S-D of 18.5 m with the beam trap moved away from the center of the detector to get the scattering data for the direct beam. These test will be referred to as the “short”, “long”, and “trans” scans, respectively. Upon completion of all three measurements at a given pressure, the load frame displaced the punches until the next target pressure was reached, and the next series of SANS tests was conducted. This process repeated until all tests had been run at all of the designated pressures. IS and SANS tests were also conducted on the test setup with no powder loaded into the die to determine the background data contributed by the setup.

The IS measurements gave the real and imaginary impedance and the impedance magnitude and phase angle at each pressure over the aforementioned frequency range. The resistivity of the powder at a given pressure was determined from the low frequency limit of the impedance magnitude, and was used in conjunction with the volume of the powder at that pressure to derive the resistivity.

After the tests were completed, the 2-D SANS data at each pressure was reduced to 1-D data using the SPICE software package developed at ORNL. There was a region of overlap in the Q values of the two 1-D data sets. Ideally, each pair of data points with the same Q should have had the same intensity, but this was not the case in our tests, in which the low-Q data from the short scan tests always had a smaller slope and less intensity than the high-Q data from the long scan tests (Fig. 3). In order to proceed

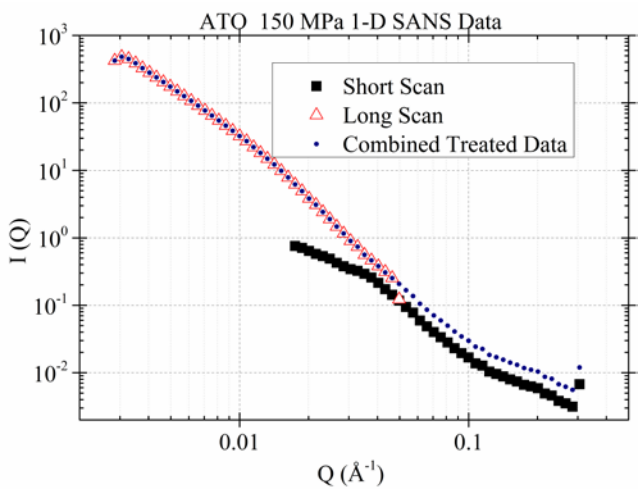


Figure 3: 1-D SANS data for the ATO nanopowder at 150 MPa applied pressure, showing the initial data for the two S-D distances and the final combined data.

with data fitting, the two 1-D data sets had to be combined into one continuous data set. This was done by first assuming that for the data with overlapping Q values, the long scan data was more accurate. Therefore, all short scan data with overlapping Q values except the 2 points with the highest Q values were removed, along with the highest-Q point of the long scan data, which had a large error in all tests. The remaining short scan data points were multiplied by a scaling factor, calculated as the intensity of the largest remaining Q point in the long scan data divided by the intensity of the smallest remaining Q point in the short scan data. This procedure translated the remaining short scan data upward to connect to the end of the remaining long scan data on the 1-D I(Q) vs Q log-log plot (Fig. 3), resulting in a single continuous data set. The data was then fitted and analyzed using the Irena software tool suite [12] for the Igor platform to determine the size, number, and volume distribution of pores, and the surface area of the microstructure. Porosity was calculated as the area under the volume distribution curve.

## 3 RESULTS AND DISCUSSION

All three powders tested in this study exhibit a sequential decrease in both impedance magnitude and resistivity with increasing applied pressure. The electrical characterization data for the compressed ATO nanopowder is presented in figure 4 as an example, which shows that the impedance magnitude at low frequencies (Fig. 4a) and the resistivity (Fig. 4b) both decrease sequentially with increasing pressure. These were the expected trends, since increased pressure improves the contact between the powder particles, thus facilitating current flow. SANS results show a consistent, sequential trend of decreasing size, number, and volume distribution of pores, as well as decreasing surface area of the microstructure and porosity, with increasing applied pressure. These trends are displayed in the cumulative surface area and porosity data plots for

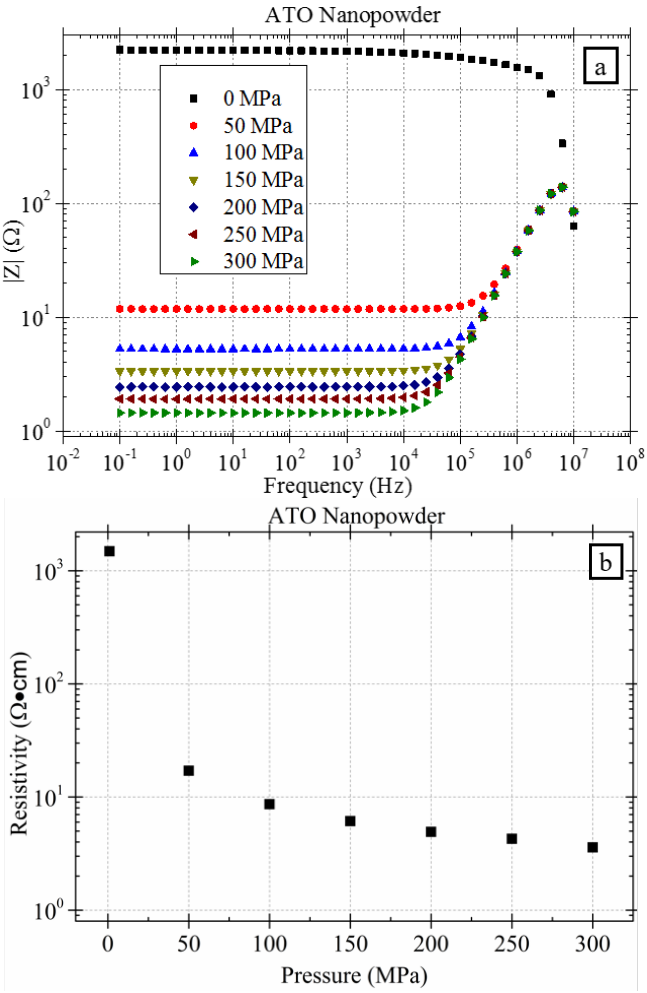


Figure 4: (a) Impedance magnitude vs log frequency and (b) resistivity as a function of applied pressure for IS measurements of the ATO nanopowder, both of which decreased sequentially with increasing applied pressure as shown.

the compressed ATO nanopowder, presented in figures 5a and 5b, respectively. These trends were also expected, since increasing the pressure on the powder forces the particles closer together. However, the porosities derived from the SANS results were far lower than expected for all three powders, with values of less than 6% at all pressures, as shown in the ATO data (Fig. 5b). If the powder particles are assumed to be spherical, the porosity should never be lower than that of the densest packing possible with monosized spheres, which is approximately 26%. Therefore, there is some problem, either in the testing process or the processing of the data, which is causing the porosity data to be much lower than the actual porosity of the powder samples. The most likely cause of this issue is the range of measured scattering angles. The smallest scattering angle measured in the SANS tests was 0.123°, which corresponds to a feature size of 0.22 µm, so data for pores with a diameter greater than 0.22 µm was not collected. Larger pores provide a larger contribution to the total porosity of the microstructure, so even if the fraction

of pores outside the range of the SANS tests was small, they may account for the majority of the total porosity. The presence of large pores also results in multiple scattering of the neutrons, which could also be affecting the interpretation of the data [1, 2].

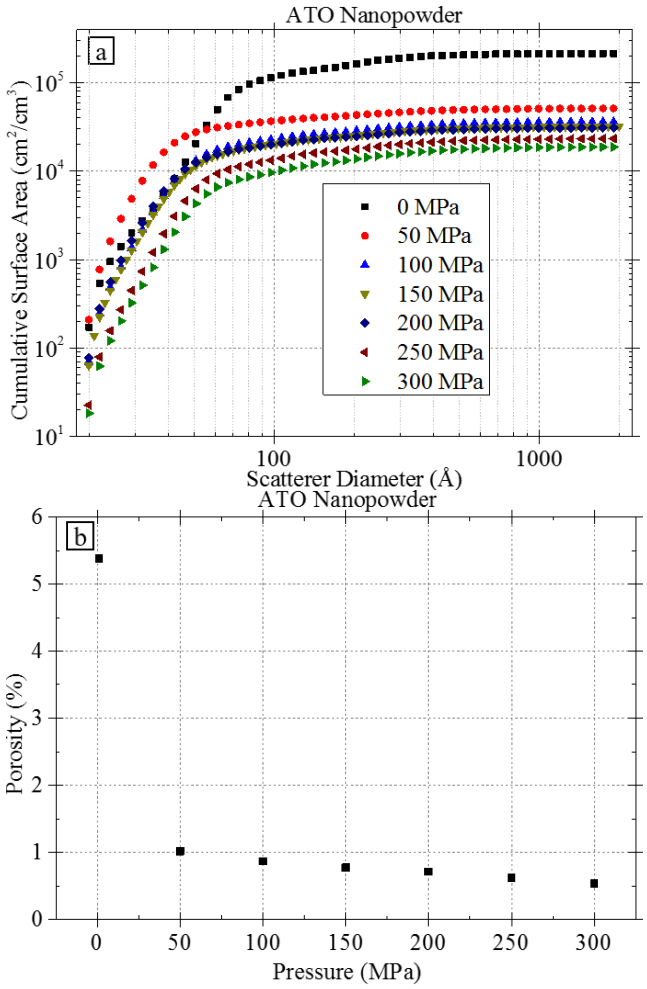


Figure 5. (a) Cumulative surface area and (b) porosity of the ATO nanopowder, both of which consistently decreased with increasing applied pressure.

## 4 CONCLUSIONS AND FUTURE WORK

Together, the facts that the IS and SANS data results follow their respective expected trends show that the test setup used in this study successfully tracked the changes in electrical and microstructural properties of the powders during compaction and was, therefore, an effective proof of concept as a powerful new characterization method. Improvements to the testing process to fix the current issues have been planned, including using USANS to gather data for larger pores by measuring smaller scattering angles and redesigning the test cell and load frame to reduce multiple scattering and the air gap between the test cell and the detector, respectively. The missing porosity in the current study should appear in the USANS results as long as the measured scattering angles are small enough to measure the largest pores in the powders. Future tests will incorporate a method for heating the powders, so this technique can be used to characterize powders during sintering.

## 5 ACKNOWLEDGEMENTS

We thank Dr. Ken Littrell at ORNL for assistance with SANS tests, Paris Cornwell at ORNL for design of the T2C fixture and die assembly, Jeff Bunn at ORNL for assistance with the load frame controls and troubleshooting, and Stephen Jesse for loaning us the impedance equipment and computer, and funding support: NSF DMR-1207323.

## REFERENCES

[1] H.M. Kerch, H.E. Burdette, R.A. Gerhardt, S. Krueger and G.G. Long, Mat.Res.Soc.Symp.Proc, 346, 177-182, 1994.

[2] G.G. Long, S. Krueger, R.A. Gerhardt and R.A. Page, J. Mat. Res., 6 [12], 2706-2715, 1991.

[3] W.D. Kingery and M. Berg, Journal of Applied Physics, 26, 1205 1955.

[4] G.G. Long, S. Krueger, P.R. Jemian, D.R. Black, H.A. Burdette, J.P. Cline and R.A. Gerhardt, J. Appl. Cryst., 23, 535-544, 1990.

[5] Jan Ilavsky, Gabrielle G. Long, Andrew J. Allen and Christopher C. Berndt, Materials Science and Engineering, A272 , 215–221, 1999.

[6] A.J. Allen, Journal of the American Ceramic Society, 88 [6], 1367-1381, 2005.

[7] T.L. Pruyn and R.A. Gerhardt. J. Am. Ceram. Soc., 98 [1], 154-162, 2015.

[8] T.L. Pruyn and R.A. Gerhardt, Advances in Bioceramics and Porous Ceramics IV: Ceramic Engineering and Science Proceedings, 32 [6], 199-210, 2011.

[9] R. A. Gerhardt, 350–363, Encyclopedia of Condensed Matter Physics, Edited by G. Bassani, G. Liedl, and P. Wyder. Elsevier, Oxford, UK, 2005.

[10] M. C. Steil, F. Thevenot, and M. Kleitz, Journal of Electrochemical Society, 144 [1] 390-98, 1997.

[11] G.D. Wignall, K.C. Littrell, W.T. Heller, Y.B. Melnichenko, K.M. Bailey, G.W.Lynn, D.A. Myles, V.S. Urban, M.V. Buchanan, D.L. Selby, and P.D. Butler, J. Appl. Cryst. 45, 990-998, 2012.

[12] J. Ilavsky and P. R. Jemian, Journal of Applied Crystallography, 42, 347-353, 2009.